

Unusual behavior in $\bar{p} - p$ and $\ell - p$ collisions involving high energy and momentum transfer: $Z^0(W^\pm)$ and scalar jets.

Saul Barshay and Georg Kreyerhoff*

III. Physikalisches Institut A
RWTH Aachen
D-52056 Aachen
Germany

December 24, 2018

Abstract

We show that the axial-vector coupling of $Z^0(W^\pm)$ to quarks, when acting together with the emission of a hypothetical spin-zero jet-generating quantum coupled to quarks results in an unusual behavior in certain processes, at high energy and momentum transfer. This involves an excess jet production at the subpicobarn level.

The purpose of this paper is to show how a general, dynamical effect can result in unusual behavior at high energy and momentum transfer, in processes which involve jet production and a real, or virtual, $Z^0(W^\pm)$. We present definite numerical examples of the effect which are applicable to $\bar{p} - p$ collisions [1], and to $\ell - p$ collisions [2], where data is being collected and analyzed. The specific motivations for emphasizing this general, dynamical phenomenon are the following.

- (1) There is a possible excess [3, 4] in the production of W plus one jet, in $\bar{p} - p$ collisions at 1.8 TeV at the Tevatron. [4].
- (2) There is also a possible excess in the production of Z plus one jet at Fermilab [5]. In determining the expectation from QCD, the precise choice of scale seems to be relevant [5].

*E-mail: georg@physik.rwth-aachen.de

- (3) There may be an excess in the production of W plus two jets at Fermilab [5].
- (4) A small excess in inclusive jet production may be present in the Tevatron experiments [1, 4, 6, 7]. The range of x -values and of p_T are rather similar to the range of these essential kinematic variables (high initial collision energy and high final transverse energy), relevant to the HERA anomalous events, the next point.
- (5) In positron-proton collisions at HERA there is a possible excess [2] in the jet production associated with deep-inelastic scattering.

In the latter experiments, the negative of the squared four-momentum transfer from the lepton is $(-Q^2) \sim (2m_Z)^2$; thus virtual $Z(W)$ exchange is comparable to virtual photon exchange. Then, the processes (1),(2),(3) and (5) all involve explicitly a massive vector boson with its axial-vector coupling to quarks, and a hadronic jet, or jets. It is of interest to examine a general, hypothetical mechanism which may be capable of giving a common physical basis for these several effects, which await experimental confirmation.

Such a general mechanism arises when the axial-vector coupling of a massive vector boson to quarks acts in a matrix element, together with the scalar (or pseudoscalar) coupling to quarks of a hypothetical spin-zero, jet-generating quantum J_0 [8,9]. The essential point is illustrated by considering the process $\bar{q} + q \rightarrow Z + J_0$. The two Feynman diagrams are shown in fig. 1. Instead of emission of the colored gluon with spin-one of QCD, we consider emission of an analogous, hypothetical spin-zero quantum, thus replacing γ_μ by 1 at the emission vertex and denoting the coupling constant by g_0 . The differential cross section is

$$\frac{d\sigma_{J_0 Z}}{dy} = \sqrt{2}G_F \left(\frac{4}{9} \frac{g_0^2}{4\pi} \right) \left(1 - \frac{m_Z^2}{4E^2} \right) \left[\frac{m_Z^2}{4E^2} \left(\frac{A}{1-y^2} - B \right) + \frac{B}{2} \right] \quad (1)$$

The total energy of the $\bar{q}-q$ annihilation is $2E$ and the emission angle of J_0 is θ , with $y = \cos \theta$, in the center-of-mass (CM) system of the $\bar{q}-q$ collision. In eq. (1), we have neglected the effective mass of the scalar quantum, as well as the quark masses. With the vector and axial-vector coupling of Z^0 to u and d quarks given by the standard model, for $\sin^2 \theta_W \sim 0.23$, $A = 4 \left((g_V^u)^2 + (g_A^u)^2 + (g_V^d)^2 + (g_A^d)^2 \right) \sim \frac{3}{2}$ and $B = 4(g_A^u)^2 + (g_A^d)^2 = \frac{5}{4}$. The Fermi constant is G_F . The elementary cross section rises sharply away from threshold at $4E^2 = m_Z^2$. The last term in the square bracket arises from the axial-vector coupling of Z . This term is responsible for an unusual behavior at very large energies. The elementary cross section does not fall as $1/E^2$. The mass m_Z brings in the natural scale, well above which unusual behavior in the form of an excess becomes predominant. For the purpose of illustrating this behavior in a transparent manner, we fold the elementary differential cross section with a simple parametrization [10] of the $\bar{q}-q$ luminosity function $(\frac{dL}{d\tau})_{u\bar{u}} = 4(\frac{dL}{d\tau})_{d\bar{d}} = \frac{2e^{-10\sqrt{\tau}}}{\tau}$. (There is time to perform folding with complete parametrizations

of quark distributions if the above experimental indications are confirmed, and if this dynamical idea proves to be useful in relating the effects.) The folding with eq. (1) results in an illustrative formula for the transverse momentum (p_T) distribution for the spin-zero jet quantum produced in $\bar{p} + p \rightarrow Z + J_0$,

$$\begin{aligned} \frac{d\sigma_{J_0 Z}}{dp_T} (\text{picobarns/GeV}) &= 8 \times 10^4 \left(\frac{g_0^2}{4\pi} \right) \frac{p_T}{s} \int_{\tau_{min}}^1 d\tau \frac{e^{-10\sqrt{\tau}}}{\tau^2} \left(1 - \frac{m_Z^2}{\tau s} \right)^{-1} \\ &\times \left[1 - \frac{4p_T^2}{\tau s \left(1 - \frac{m_Z^2}{\tau s} \right)^2} \right]^{-\frac{1}{2}} \left\{ \frac{3}{32} \frac{m_Z^2}{p_T^2} \left(1 - \frac{m_Z^2}{\tau s} \right)^2 - \frac{5}{16} \left(\frac{m_Z^2}{\tau s} - \frac{1}{2} \right) \right\} \end{aligned} \quad (2)$$

with $\tau_{min} = (p_T + \sqrt{p_T^2 + m_Z^2})^2/s$. The scalar jet quantum J_0 could break up via two gluons; therefore it could exhibit a tendency to materialize into hadrons as two (correlated) jets. For this reason, we have used for the elementary cross section the full formula including the squared, effective mass, $m_{J_0}^2$, of the complete hadronic system which results from the break-up and fragmentation of the spin-zero quantum J_0 . This is given by^{F1}

$$\begin{aligned} \frac{d\sigma_{J_0 Z}}{dy} &= \sqrt{2} G_F m_Z^2 \frac{4}{9} \frac{g_0^2}{4\pi} \frac{\left(x^2 - \frac{m_{J_0}^2}{4E^2} \right)^{\frac{1}{2}}}{E^2} \left[(A+B) \left(\frac{1}{D^2} + \frac{1}{\bar{D}^2} \right) (1-y^2) \right. \\ &\times \left(E^4 x^2 - E^2 m_{J_0}^2 \right) + 2(A-B) \frac{1}{D\bar{D}} \left(E^4 x^2 (1-y^2) + E^2 m_{J_0}^2 y^2 \right) \\ &+ 2(A+B) \left(\frac{(u^2 - m_{J_0}^2 u + \frac{m_{J_0}^4}{4})}{D^2} + \frac{(v^2 - m_{J_0}^2 v + \frac{m_{J_0}^4}{4})}{\bar{D}^2} \right) \left(\frac{E^2}{m_Z^2} \right) \\ &\left. + 4(A-B) \frac{(uv - \frac{m_{J_0}^2}{2}(u+v) + \frac{m_{J_0}^4}{4})}{D\bar{D}} \left(\frac{E^2}{m_Z^2} \right) \right] \end{aligned} \quad (3)$$

with

$$\begin{aligned} D &= (2u - m_{J_0}^2) & \bar{D} &= (2v - m_{J_0}^2) \\ u &= E^2 x \left(1 - \left(x^2 - \frac{m_{J_0}^2}{E^2} \right)^{1/2} \left(\frac{y}{x} \right) \right) & v &= E^2 x \left(1 + \left(x^2 - \frac{m_{J_0}^2}{E^2} \right)^{1/2} \left(\frac{y}{x} \right) \right) \\ x &= \left(1 + \frac{m_{J_0}^2}{4E^2} - \frac{m_Z^2}{4E^2} \right) & y &= \cos \theta \end{aligned}$$

In fig. 3, we exhibit the p_T -distribution $\frac{d\sigma_{J_0 Z}}{dp_T}$ at $\sqrt{s} = 1.8$ TeV and in fig. 3 the p_T -distribution at $\sqrt{s} = 630$ GeV, for several values of $m_{J_0}^2$. Solely for comparison,

^{F1}The present results correct the cross-section formulae in ref. [9]

we have also shown in figs. 2,3 the p_T -distribution $\frac{d\sigma_{gZ}}{dp_T}$ for $\bar{p}+p \rightarrow Z^0+g$, calculated approximately from the elementary cross section (with $m_g^2 = 0$)

$$\begin{aligned} \frac{d\sigma_{gZ}}{dp_T} &= \sqrt{2}G_F \frac{4}{9}\alpha_s(p_T) \left(1 - \frac{m_Z^2}{4E^2}\right)^{-1} \frac{(A/2)}{(1-y^2)} \\ &\times \left(\left(1 + \frac{m_Z^2}{2E^2}\right)^2 + \left(1 - \frac{m_Z^2}{4E^2}\right)^2 y^2 \right) \end{aligned} \quad (4)$$

In this illustrative numerical work, we use a fixed scalar coupling, $\frac{g_0^2}{4\pi} \sim 2(\alpha_s(m_Z))^2 \sim 0.025$; and for g , we use the decreasing (with scale p_T) coupling $\alpha_s(p_T^2) \sim \frac{1.64}{\ln(25p_T^2)}(1 - \frac{0.66 \ln(\ln(25p_T^2))}{\ln(25p_T^2)})$, ($\Lambda = 200$ MeV). From the figures, one can follow the onset of a relatively significant contribution to the differential cross section, at the subpicobarn per GeV level. This occurs for p_T above $\sim m_Z$. The more flat p_T -distribution in production of J_0 reflects the more flat angular distribution in the CM of the basic $\bar{q}-q$ -collision process. The enhancement at quite large $p_T > 2m_Z$, is substantial. However, the level of the cross section is then very low, $< 10^{-1}$ pb/GeV. The quark vertex for an effective scalar quantum may involve two-gluon structure; in any case, damping is to be expected, at high energies, for emission of J_0 with very large momenta, thus reducing this cross section. In fig. 4, at $\sqrt{s} = 1.8$ TeV, we plot the p_T -distribution $\frac{d\sigma_{J_0Z}}{dp_T}$ for the case in which $\left(\frac{g_0^2}{4\pi}\right)$ is taken as decreasing like $(\alpha_s(p_T/2))^2$, instead of being a fixed number ~ 0.025 , as in fig. 2. Such a “running” coupling strength implies, of course, a non-perturbative domain at low momenta (see footnote F2 below). From fig. 4 (relative to fig. 2), one notes an increase in the p_T at which excess jet production begins to stick out prominently, to $p_T \sim 1.5m_Z$, and a reduction in the cross section. In fig. 6, we plot an integrated cross section $\sigma_{J_0Z} = \int_a^b dp_T (\frac{d\sigma_{J_0Z}}{dp_T})$ versus \sqrt{s} , where we use $a = 50$ GeV and where $b = (p_T)_{max} = \left\{ \left(\frac{s+m_{J_0}^2-m_Z^2}{2\sqrt{s}} \right)^2 - m_{J_0}^2 \right\}^{1/2}$. This cross section is shown for the several values of $m_{J_0}^2$. At $\sqrt{s} = 1.8$ TeV, $\sigma_{J_0Z} \lesssim \sigma_{gZ}/2$; thus the integrated effect is not large. (The detailed expectation from g alone has a comparable uncertainty arising from the choice of scale [5], and the present data have a similar uncertainty [5].)

We are motivated to examine the possible role of this dynamical mechanism in bringing about unusual behavior in deep-inelastic lepton-nucleon scattering (DIS) by the following considerations. For neutral-current DIS, the relevant Feynman diagrams are shown in fig. 8. The $(-Q^2)$ must be sufficiently large in order to make the matrix element from exchange of a virtual Z^0 comparable to that from exchange of a virtual photon. This brings in the sizable axial coupling of Z^0 to quarks. Concerning the other two relevant variables [2]:

- (1) the scaled energy loss from the lepton, in the rest system of the proton, y ($0 \leq y \leq 1$), tends to be preferentially large because of the explicit momentum

factor in the phase space for J_0 , which favors backward scattered electrons in the laboratory, (this is so in a perturbative domain, $(\frac{g_0^2}{4\pi}) \ll 1$).^{F2}

- (2) the intermediate-state quark lines in fig. 8 involve, in general, virtual quarks, not mass-shell quarks with m^2 taken as zero. For diagram (a), in particular, this means $(Q + q_i)^2 = (p_{J_0} + q)^2 \geq 0$. Thus, $2Q \cdot q_i \geq (-Q^2)$, which converts into $(xy) \geq \frac{(-Q^2)}{s}$ ($\sqrt{s} = 300$ GeV at HERA; the present excess of events [2] involve $(-Q^2) \approx (2m_Z)^2$). Since $y_{max} = 1$, x must be greater than 0.36. The value of x is then determined by the effective invariant mass of the all of the hadrons that are to be included in the final-state system (jet or jets, plus possible relatively widely-spread, softer systems^{F2}).

Calculation of the squared matrix element arising from the two diagrams in fig. 8 exhibits a dominant piece involving only the axial-vector coupling, with the form^{F3}

$$2 \left(2(g_A^u)^2 + (g_A^d)^2 \right) \sim 1 \quad (5)$$

The term causes an analogous unusual behavior to that encountered in the process $\bar{q} + q \rightarrow Z + J_0$. It brings in an excess of jet production which can become noticeable when values of $(-Q^2) \gg m_Z^2$ are attained, because the axial-vector coupling comes to the fore. A rough estimate indicates a cross section significantly less than 0.1 pb at the quark level^{F4}, using the small number $(\frac{g_0^2}{4\pi}) \sim 0.025$. A more significant effect requires increasing this number, at least for low momenta^{F2} of a hypothetical scalar quantum^{F5}. Therefore, it is worth emphasizing that there are general issues connected with the possibility of dynamical jet enhancement. One concerns the characteristics of the hadronic jet, or jets - that is the kinematic aspects of all of hadrons included in this system. Are there aspects of these hadrons which differ from jets arising from single, ordinary quarks? In particular, production of J_0 together with the quark, in an overlapping jet structure, can give rise to a significant spreading of particles in the $(x - z)$ plane (or in the $(y - z)$ plane), that is in pseudorapidity; also a spreading in $(x - y)$ plane, that is in azimuthal angle. The possibility that a spin-zero, jet-producing quantum breaks down via two gluons is a motivation to look for unusual multi-jet structure - three jets in $\ell - p$ DIS; four jets in e^+e^- annihilation. There can be a significant component of heavy quarks associated

^{F2}If a nonperturbative domain occurs for very low momenta of a scalar quantum, then the condition $xy \rightarrow \frac{-Q^2}{s}$ with $(-Q^2) \gg m_Z^2$ as the relevant physical condition for bringing Z -exchange and the axial-vector coupling to the fore, tends to favor the larger values of x for which a significant initial quark flux is still present; thus also large values of y .

^{F3}The matrix elements from the two diagrams in fig. 8 interfere. There is a prominent piece when the intermediate-state quark lines have a comparable virtuality, that is, $(Q + q_i)^2 \sim -(q_i - p_{J_0})^2$.

^{F4}A cross section of 0.1 pb may be considered as the smallest value which can explain the most notable of the anomalous events in the experiments of ref. [2]; that is, the two events in each experiment which have $(-Q^2) > 30000 (\text{GeV})^2 \sim (2m_Z)^2$.

^{F5}This may suggest an effective scalar coupling strength which “runs” upward to of order unity in a non-perturbative domain at low p_{J_0}

with J_0 . Perhaps the “bottom” line of these considerations is that the nature of the jet structure associated with possible anomalous behavior at high energy and momentum transfer, must be investigated in the data.

In processes involving “strong” interactions alone, J_0 production gives rise to an increased inclusive jet production. The effect need not be dramatic [4]. As an illustration, in fig. 7 ($\sqrt{s} = 1.8$ TeV) and fig. 8 ($\sqrt{s} = 630$ GeV) we examine additional two-jet processes by plotting a ratio of differential cross sections $R(p_T, \sqrt{s})$ versus p_T , where

$$R(p_T, \sqrt{s}) = \frac{\left(\frac{d\sigma(J_0, g)}{dp_T} + \frac{d\sigma_q(g, g)}{dp_T} \right)}{\frac{d\sigma_q(g, g)}{dp_T}} \quad (6)$$

The process $\bar{q} + q \rightarrow J_0 + g$ utilizes eq. (1) with $m_Z^2 \rightarrow 0$; the process $\bar{q} + q \rightarrow g + g$ utilizes eq. (4) with $m_Z^2 \rightarrow 0$ (and with appropriate coupling parameters and color factors). The axial-vector couplings are absent. The fixed coupling $\left(\frac{g_0^2}{4\pi} \right)$ is taken as 0.025, and $\alpha_s(p_T)$ decreases with increasing p_T . Note that if, at $\sqrt{s} = 630$ GeV, one were to renormalize R to unity at a value of the scaled variable $x_T \sim 0.35$ ($E_T \sim 110$ GeV), then at the same x_T , the quantity is above unity at $\sqrt{s} = 1.8$ TeV ($E_T \sim 315$ GeV). Observe behavior of this kind in preliminary data in figs. 10 and 11 of ref. 7. The presence of scalar quanta can make the gluon coupling strength $\alpha_s(p_T)$ appear to “run” downward more slowly, when data is parameterized by $\alpha_s(p_T)$ alone. In fig. 9, we show $R(p_T, \sqrt{s} = 1.8 \text{ TeV})$ for the case in which $\left(\frac{g_0^2}{4\pi} \right)$ is taken as decreasing like $(\alpha_s(p_T/2))^2$. Corresponding considerations can be made for the process of production of direct photons plus one and two jets. Certain discrepancies exist in preliminary data at the Tevatron [11]; in particular, note section 4 of ref. 11 concerning two jets. A general consideration is that correlation of two jets originating in a scalar quantum can reduce the relative occurrence of the larger transverse momenta of a jet, as measured relative to the effective mass of the full photon-jet-jet system. There can be an excess of events at low momenta (mass).

We conclude by simply noting that the present experimental indications for “non-standard” behavior in certain processes at high energy and momentum transfer, which involve hadronic jets in the final state, may be correlated^{F6}. The reason for this lies in the possibility that the jet production itself involves new dynamics, rather than being a secondary product of the production of many [12] exotic particle states [2].

^{F6}To our knowledge, the present work is the only paper which addresses the possibility of a new physical connection between several tentative, unusual effects at the Tevatron, and the apparently anomalous behavior at HERA. We have become aware of a recent paper, ref. [13], which discusses some of the Tevatron data and the HERA data. This paper involves additional precise adjustment (in which the authors are authorities) of the parton distributions at large x , with an unusual form, so that the usual QCD calculations produce “excess” events at high energy and p_T . This is, in a sense, complementary to the present work, where we have considered new dynamics in the elementary cross sections, and have used a qualitative parton flux for illustration of the physical effects. (See also ref. [14], involving leptoquarks.)

One author (S. B.) thanks Paolo Giromini for communications from Fermilab. This author also thanks Patrick Heiliger for help.

References

- [1] CDF Collaboration, F. Abe et al., Phys. Rev. Lett. **77** (1996) 438
- [2] H1 Collaboration, C. Adloff et al., DESY 97-24 (February, 1997) (hep-ex/9702012).
ZEUS Collaboration, J. Breitweg et al., DESY 97-025 (February, 1997) (hep-ex/9702015)
- [3] D0 Collaboration, S. Abachi et al., Phys. Rev. Lett. **75** (1995) 3226
- [4] R. Brock, *High p_T physics: results from the Tevatron*, Proceedings of the International Conference on High-Energy Physics, Warsaw, 1996.
- [5] Private communications from Paolo Giromini concerning data of the CDF Collaboration, which is under analysis.
- [6] E. Buckley-Geer, for CDF and D0 Collaborations, Fermilab-Conf-96/345-E (September 1996)
- [7] B. Flaughner, for CDF Collaboration, Fermilab-Conf-96/225-E (August, 1996).
- [8] S. Barshay, O. Miyamura and T. Hashimoto, Phys. Lett. **155B** (1985) 77
- [9] S. Barshay and A. van Proeyen, Phys. Lett. **83B** (1979) 230.
- [10] R. Cahn, LBL report-15469 (1982)
- [11] L. Modulman, for the CDF Collaboration, Fermilab-Conf-96/337-E (October, 1996)
- [12] K. S. Babu, C. Kolda, J. March-Russell and F. Wilczek, IASSNS-HEP-97-04 (March 1997), hep-ph/9703299.
M. Suzuki, LBNL-40111 (March, 1997), hep-ph/9703316
- [13] S. Kuhlmann, H. L. Lai, and W. K. Jung, MSU-HEP-70316, CTEQ-705 (April 1997) (hep-ph/9704338)
- [14] I. Montvay, DESY-97-058 (April, 1997), (hep-ph/9704280).

Figures

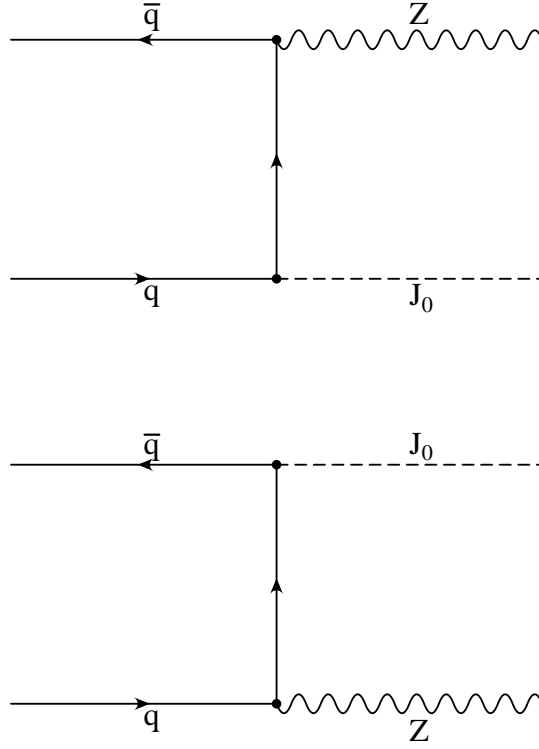


Figure 1: Feynman diagrams for the process $\bar{q} + q \rightarrow Z + J_0$. The interference between the two diagrams is instrumental in giving unusual behavior in the cross section due to the axial-vector coupling to quarks of Z .

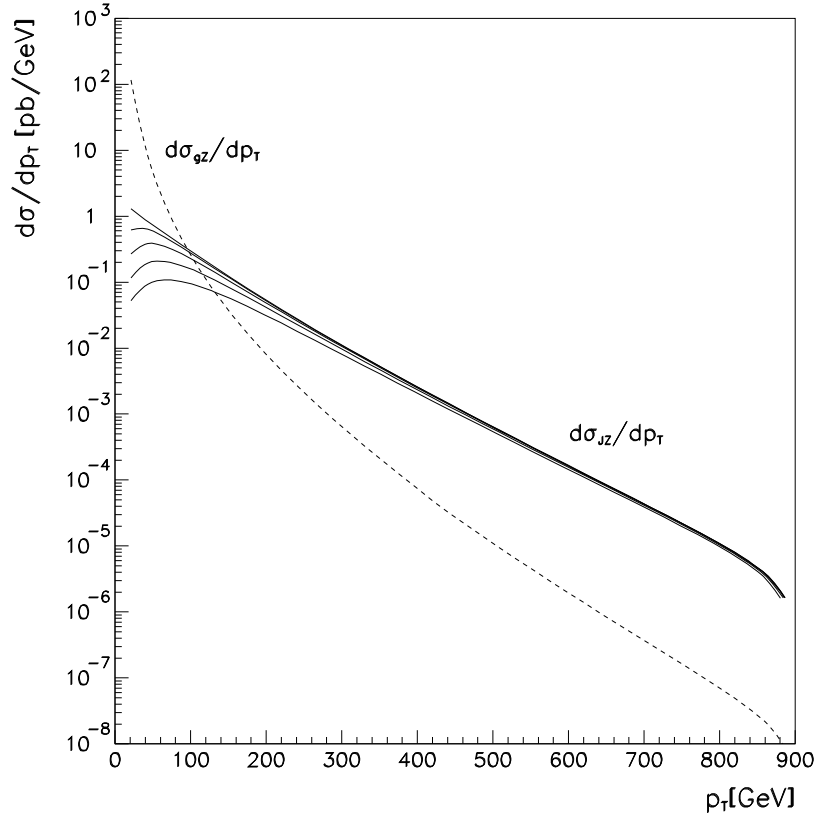


Figure 2: The solid curve gives $d\sigma_{J_0 Z}/dp_T$ versus p_T for $\bar{p} + p \rightarrow Z + J_0$ at $\sqrt{s} = 1.8$ TeV. $\left(\frac{g_0^2}{4\pi}\right) = 0.025$. Five values of the effective mass of the hadronic jet from J_0 are considered: $m_{J_0} = 0, 30, 60, 100$ and 150 GeV, reading from the upper curve to the lower. Solely for comparison, the dashed curve gives $d\sigma_{gZ}/dp_T$ for $\bar{p} + p \rightarrow Z + g$ at $\sqrt{s} = 1.8$ TeV, as calculated approximately in the text ($m_g^2 = 0$).

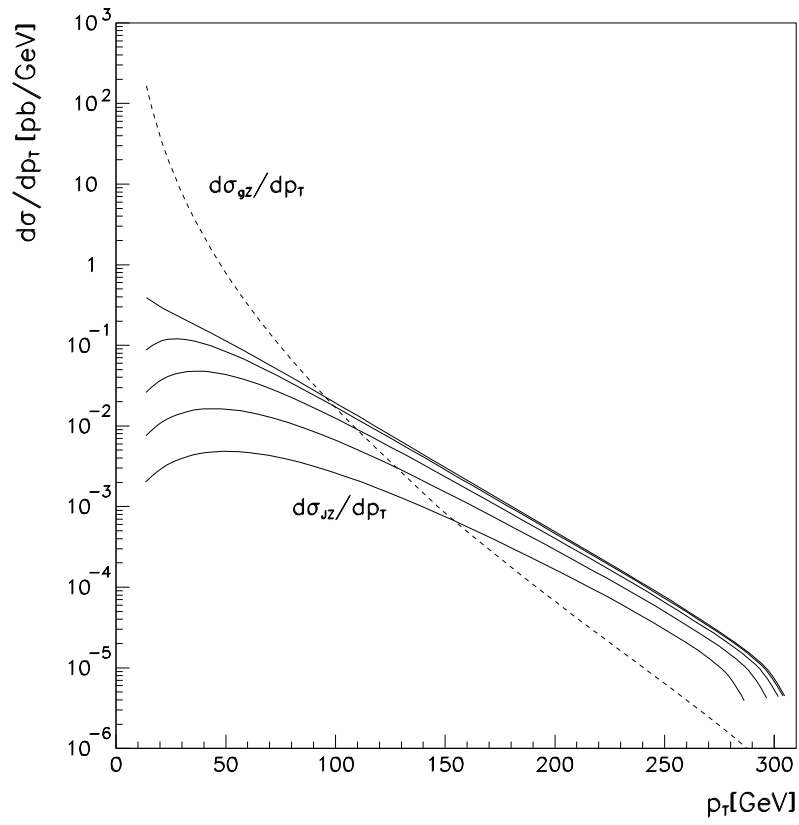


Figure 3: The same as in fig. 2, but at $\sqrt{s} = 630$ GeV.

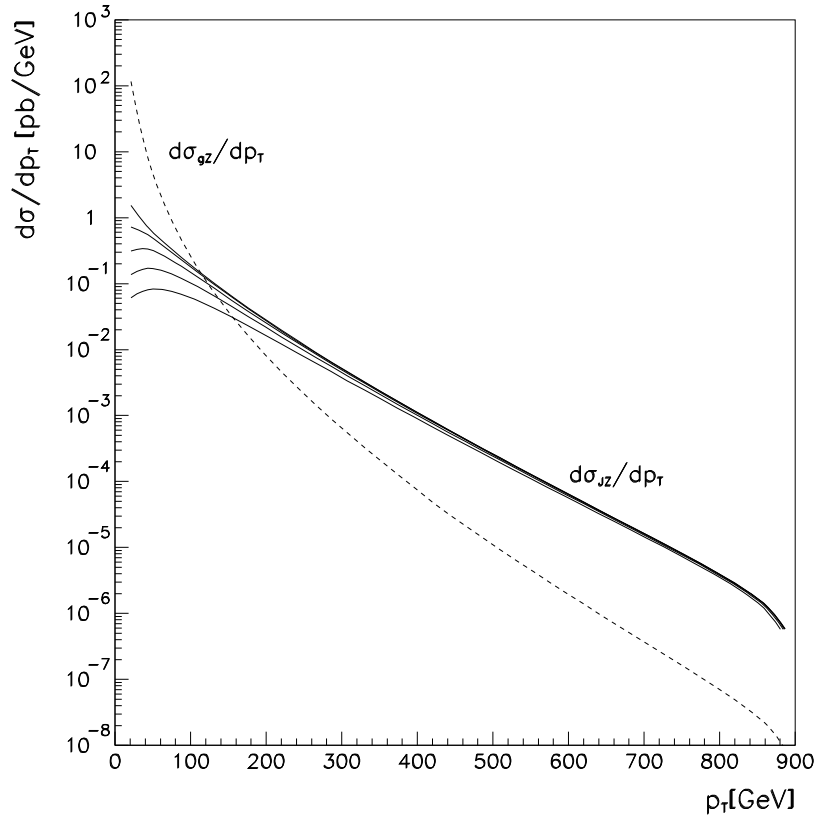


Figure 4: The same as in fig. 2, but with $\left(\frac{g_0^2}{4\pi}\right)$ taken as a function decreasing like $(\alpha_s(p_T/2))^2$ for increasing scale p_T .

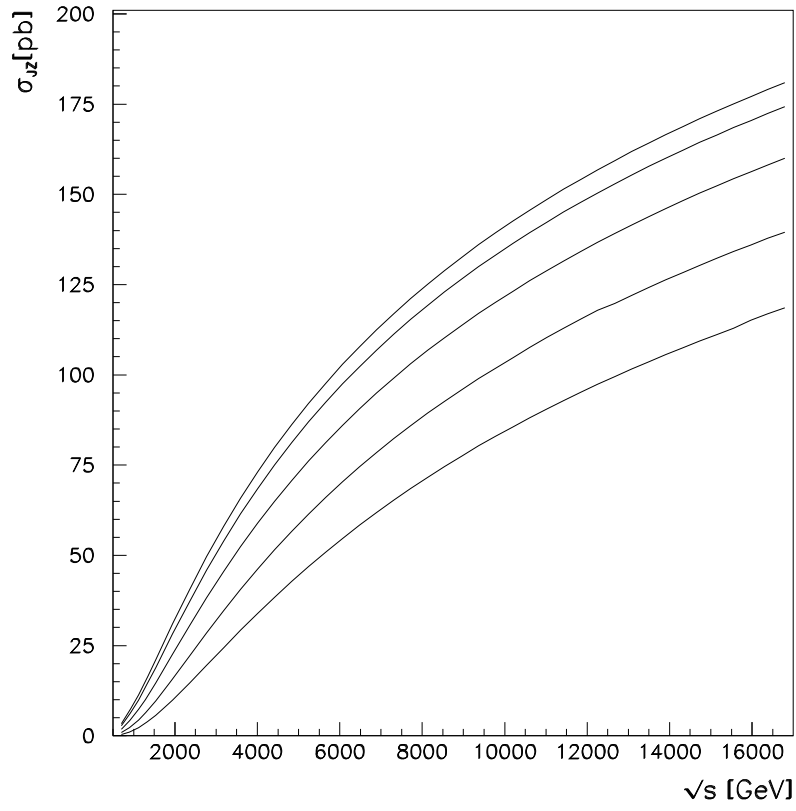


Figure 5: An integrated cross section $\sigma_{J_0 Z}(s) = \int_a^b dp_T (\frac{d\sigma_{J_0 Z}}{dp_T})$ versus \sqrt{s} , for $a = 50$ GeV, $b = (p_T)_{max} = \left\{ \left(\frac{s+m_{J_0}^2-m_Z^2}{2\sqrt{s}} \right)^2 - m_{J_0}^2 \right\}^{1/2} \cdot \left(\frac{g_0^2}{4\pi} \right) = (\alpha_s(p_T/2))^2$.

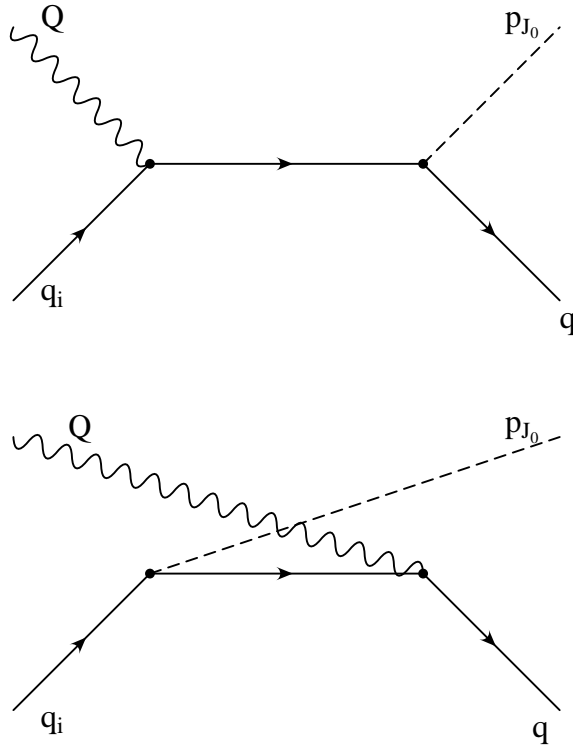


Figure 6: Feynman diagrams relevant to Z -exchange in deep-inelastic lepton-nucleon scattering. The four-momenta of the quanta are indicated. A virtual Z with high $(-Q^2)$ is exchanged to an initial quark with q_i ($q_i^2 \approx 0$). The final-state contains J_0 with p_{J_0} , and a quark with q ($q^2 \approx 0$).

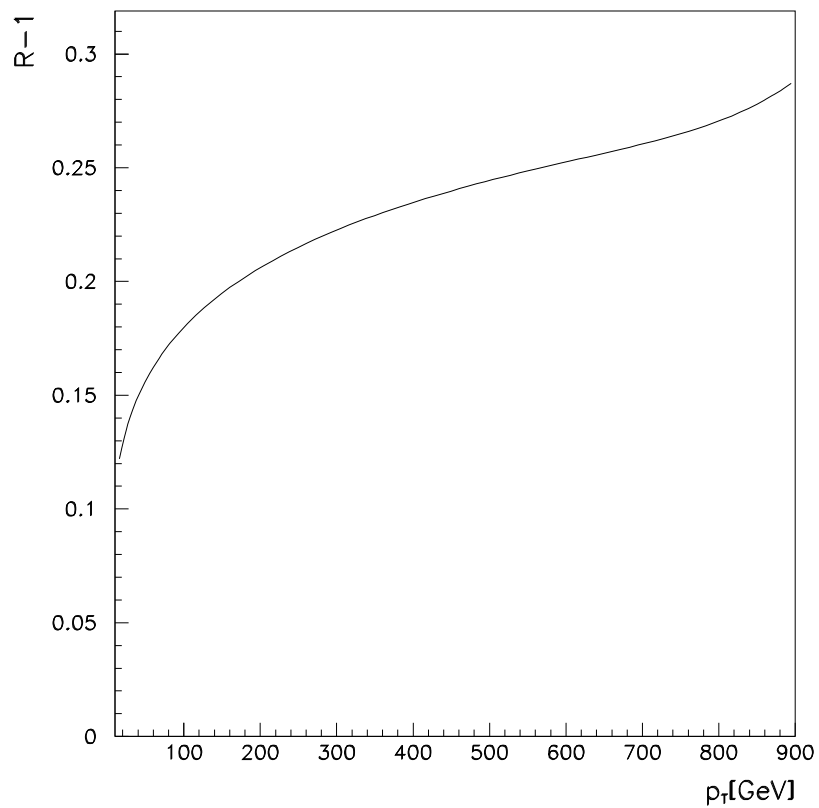


Figure 7: The ratio of differential cross sections, $R(p_T, \sqrt{s})$ given in eq. (6) of the text, at $\sqrt{s} = 1.8$ TeV, using $\left(\frac{g_0^2}{4\pi}\right) \sim 0.025$. The rise of R above unity provides an estimate of an excess inclusive jet cross section.

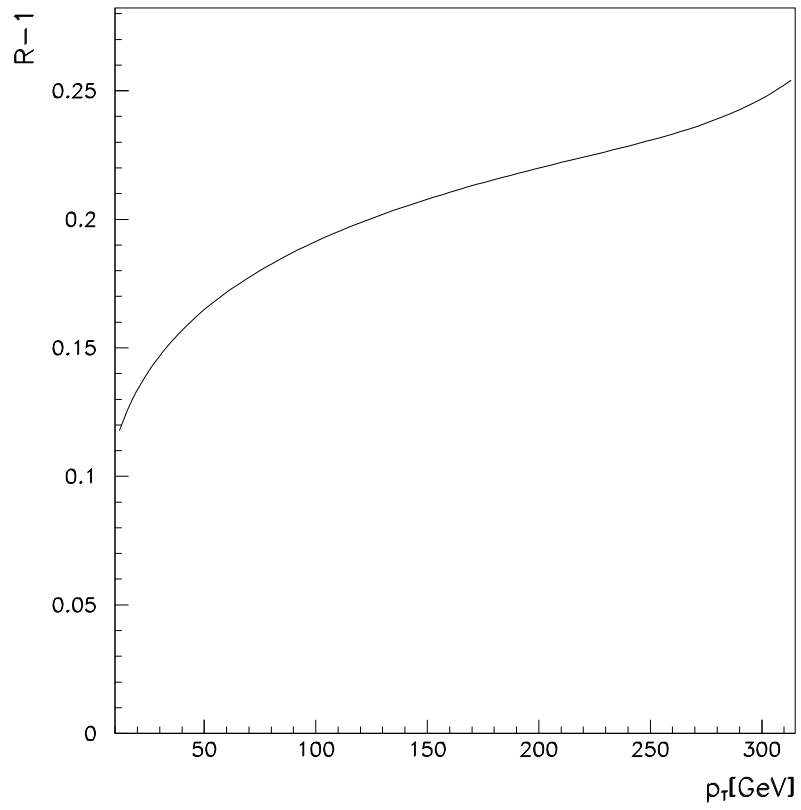


Figure 8: The same as in fig. 9, but at $\sqrt{s} = 630$ GeV.

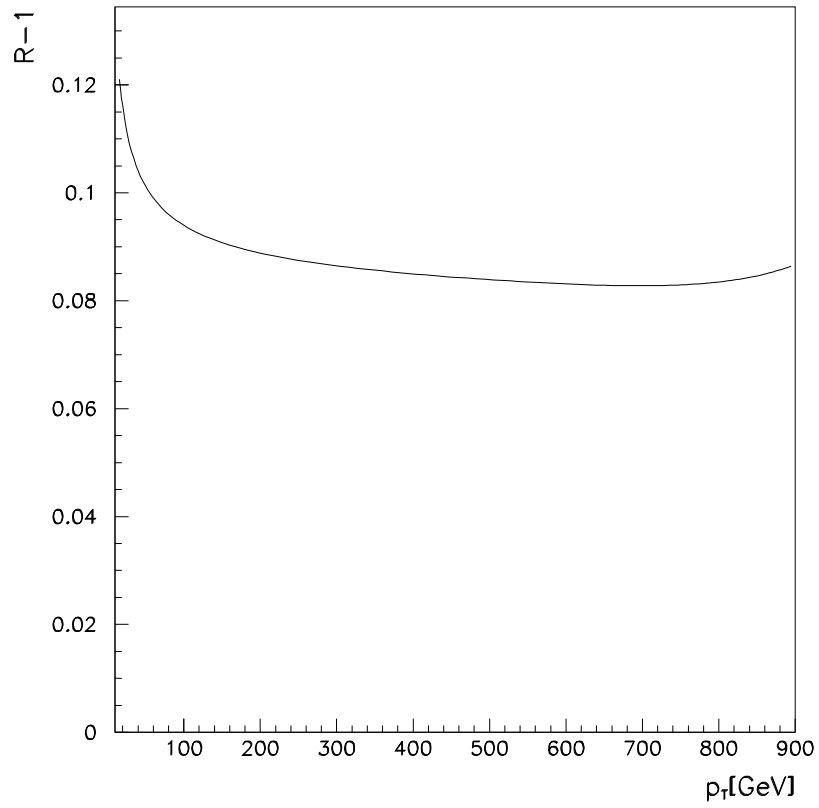


Figure 9: The ratio $R(p_T, \sqrt{s})$ at $\sqrt{s} = 1.8$ TeV, but with $\left(\frac{g_0^2}{4\pi}\right)$ taken as a function decreasing like $(\alpha_s(p_T/2))^2$ for increasing scale p_T .